Double trouble

Prajapati, Bimal; Bernal-Cabas, Margarita; Lopez-Alvarez, Marina; Schaffer, Marc; Bartel, Jurgen; Rath, Hermann; Steil, Leif; Becher, Dorte; Volker, Uwe; Mader, Ulrike

Published in:
Biochimica et Biophysica Acta (BBA) - Molecular Cell Research

DOI:
10.1016/j.bbamcr.2020.118914

Publication date:
2021

BBA - Molecular Cell Research 1868 (2021) 118914

Contents lists available at ScienceDirect

BBA - Molecular Cell Research

journal homepage: www.elsevier.com/locate/bbamcr

Double trouble: *Bacillus* depends on a functional Tat machinery to avoid severe oxidative stress and starvation upon entry into a NaCl-depleted environment

Bimal Prajapati [a], Margarita Bernal-Cabas [a], Marina López-Álvarez [a], Marc Schaffer [b], Jürgen Bartel [c], Hermann Rath [b], Leif Steil [b], Dörte Becher [c], Uwe Völker [b], Ulrike Mäder [b,*], Jan Maarten van Dijl [a,**]

[a] University of Groningen, University Medical Center Groningen, Department of Medical Microbiology, Groningen, the Netherlands
[b] University Medicine Greifswald, Interfaculty Institute of Genetics and Functional Genomics, Department of Functional Genomics, Greifswald, Germany.
[c] University of Greifswald, Institute of Microbiology, Department of Microbial Proteomics, Greifswald, Germany.

ARTICLE INFO

Keywords:
Twin-arginine translocation
Bacillus subtilis
Protein secretion
Oxidative stress
EfeB
QcrA

ABSTRACT

The widely conserved twin-arginine translocases (Tat) allow the transport of fully folded cofactor-containing proteins across biological membranes. In doing so, these translocases serve different biological functions ranging from energy conversion to cell division. In the Gram-positive soil bacterium *Bacillus subtilis*, the Tat machinery is essential for effective growth in media lacking iron or NaCl. It was previously shown that this phenomenon relates to the Tat-dependent export of the heme-containing peroxidase EfeB, which converts Fe^{2+} to Fe^{3+} at the expense of hydrogen peroxide. However, the reasons why the majority of *tat* mutant bacteria perish upon dilution in NaCl-deprived medium and how, after several hours, a sub-population adapts to this condition was unknown. Here we show that, upon growth in the absence of NaCl, the bacteria face two major problems, namely severe oxidative stress at the membrane and starvation leading to death. The *tat* mutant cells can overcome these challenges if they are fed with arginine, which implies that severe arginine depletion is a major cause of death and resumed arginine synthesis permits their survival. Altogether, our findings show that the Tat system of *B. subtilis* is needed to preclude severe oxidative stress and starvation upon sudden drops in the environmental Na^+ concentration as caused by flooding or rain.

1. Introduction

Bacterial twin-arginine translocation (Tat) pathways can translocate fully folded cargo proteins across the cytoplasmic membrane [1,2,89]. Cargo proteins that are to be translocated by Tat must contain a twin-arginine "RR"-motif in the N-terminal region of their signal peptide for specific recognition by the Tat translocase [3,4]. The *Bacillus* Tat translocation system is composed of so-called TatA and TatC subunits. TatC is the larger of the two, representing an integral membrane protein with six transmembrane domains. The smaller TatA subunit has a single N-terminal transmembrane spanning domain [5]. According to current models for protein translocation via the Tat pathway in bacteria and the thylakoidal membrane of chloroplasts, the TatA and TatC subunits of *Bacillus* collectively form a docking complex for cargo proteins [1]. The translocation process is initiated when a protein with the correct RR-signal peptide interacts with this docking complex. During the initial interaction, the docking complex proofreads the signal peptide and inserts the substrate into the membrane, which requires the recruitment of additional TatA subunits. These may either form a transmembrane pore or weaken the membrane, thereby facilitating translocation of the cargo protein [6,7]. The energy to drive the subsequent cargo translocation across the bacterial and thylakoidal membranes is provided by the proton-motive force [5,8–10]. Once the translocation process has been initiated, the signal peptide is proteolytically removed from the cargo

* Correspondence to: U. Mäder, University Medicine Greifswald, Interfaculty Institute of Genetics and Functional Genomics, Department of Functional Genomics, Felix-Hausdorff-Str. 8, 17475 Greifswald, Germany.
** Correspondence to: J. M. van Dijl, University of Groningen, University Medical Center Groningen, Department of Medical Microbiology, Hanzeplein 1 – EB80, 9700RB Groningen, the Netherlands.
E-mail addresses: ulrike.maeder@uni-greifswald.de (U. Mäder), j.m.van.dijl01@umcg.nl (J.M. van Dijl).

https://doi.org/10.1016/j.bbamcr.2020.118914
Received 23 June 2020; Received in revised form 8 November 2020; Accepted 20 November 2020
Available online 25 November 2020

protein by signal peptidase [11–13], allowing release of the translocated protein at the *trans* side of the membrane [14].

Of note, the genes for three TatA and two TatC subunits have been identified in the *B. subtilis* genome. The *tatAy-tatCy* and *tatAd-tatCd* genes are organized in operons at different genomic loci, and the *tatAc* gene is independently expressed from a third genomic locus [15]. Comprehensive expression studies have shown that the *tatAyCy* operon is constitutively expressed across many different conditions, and the same is true for *tatAc* [16]. In contrast, the *tatAdCd* operon is expressed only under conditions of phosphate limitation [15,17]. The operon-encoded Tat subunits assemble into two distinct Tat translocases: TatAyCy and TatAdCd. Each pathway works independently from the other and translocates its own cargo proteins [11,15]. While TatAdCd translocates only the phosphodiesterase PhoD, TatAyCy is known to translocate the heme-containing Dyp-type peroxidase EfeB [11,18], the Rieske iron-sulfur protein QcrA [19], and the metallo-phosphoesterase YkuE [16,19,20]. The third TatA protein, TatAc, is a dispensable component of the TatAyCy translocase, which enhances this translocase's efficiency when the function of TatAy is compromised [19]. Based on these previous observations, it has been concluded that TatAyCy represents the core Tat translocase of *Bacillus*.

While the Tat system is not essential for *B. subtilis* under most growth conditions, we observed previously that TatAyCy is very important for growth in Lysogeny Broth (LB) lacking NaCl [21,22]. When grown in LB without NaCl, mutant strains lacking *tatAy*, *tatCy* or both these *tat* genes will initially start growing. However, in the early exponential growth phase, the mutant bacteria will stop growing and lyse. Nonetheless, part of the population of mutant bacteria will adapt to the salt-deprived condition and resume growth. The severity of this growth defect depends on the degree at which TatAyCy function is affected in the export of its main substrate EfeB, as was previously shown by investigations on TatAy proteins with site-specific mutations [5]. Accordingly, *efeB* mutant *B. subtilis* cells show exactly the same phenotype in LB without NaCl as *tatAyCy* mutant cells.

The peroxidase EfeB is a subunit of the elemental iron transport complex EfeUOB in *B. subtilis* (Fig. 1), where it oxidizes ferrous iron to ferric iron at the expense of hydrogen peroxide. The lipoprotein EfeO binds the ferric iron and transfers it to the ferric iron permease EfeU in the membrane [18]. Although the need for TatAyCy-dependent translocation of EfeB across the membrane for unimpaired growth of *B. subtilis* in LB without NaCl was previously documented, the reason(s) why the *tatAyCy* or *efeB* mutant cells start to lyse in this growth condition remained unclear. In addition, it remained unclear how the surviving cells manage to recover from the lysis phase as depicted in Fig. 2. Of note, previous research had shown that the recovery of *tat* or *efeB* mutant bacteria reflects an adaptation rather than the emergence of suppressor mutations, because the cells that had resumed growth showed exactly the same lysis-recovery pattern when used to inoculate fresh LB medium without NaCl [5,21,22].

The objective of the present study was to elucidate the reasons why *tat* mutant bacteria start to lyse in the absence of NaCl, and how they manage to adapt to this condition. To address these questions, we followed an initial transcriptomics approach combined with subsequent functional verification. In brief, the results unveil a scenario where oxidative stress in the cell membrane of *tat*-deficient cells hinders the uptake of nutrients, causing the cells to starve, which ultimately leads to cell lysis. The surviving cells recover by catabolizing amino acid pools in the cell, especially arginine, and by upregulating various mechanisms to counteract the oxidative stress.

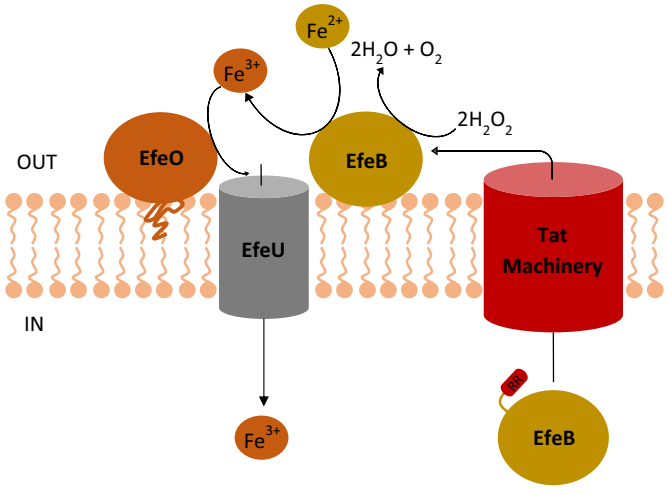

Fig. 1. Schematic representation of the EfeUOB elemental iron transport system and the Tat translocase in the membrane of *B. subtilis*. The cartoon depicts the Tat-dependent export of the ferrous iron peroxidase EfeB, which catalyzes the conversion of Fe^{2+} to Fe^{3+} at the expense of hydrogen peroxide. The newly formed Fe^{3+} is bound by the lipoprotein EfeO and transferred to the Fe^{3+} permease EfeU for uptake by the cell. EfeB and EfeO are associated with EfeU [18].

2. Materials and methods

2.1. Bacterial strains, media and basic growth conditions

Bacterial strains used in this study are listed in Supplementary Table S1. Lysogeny Broth (LB) was composed of 1% tryptone and 0.5% yeast extract with or without 1% NaCl. Bacteria were grown in LB broth

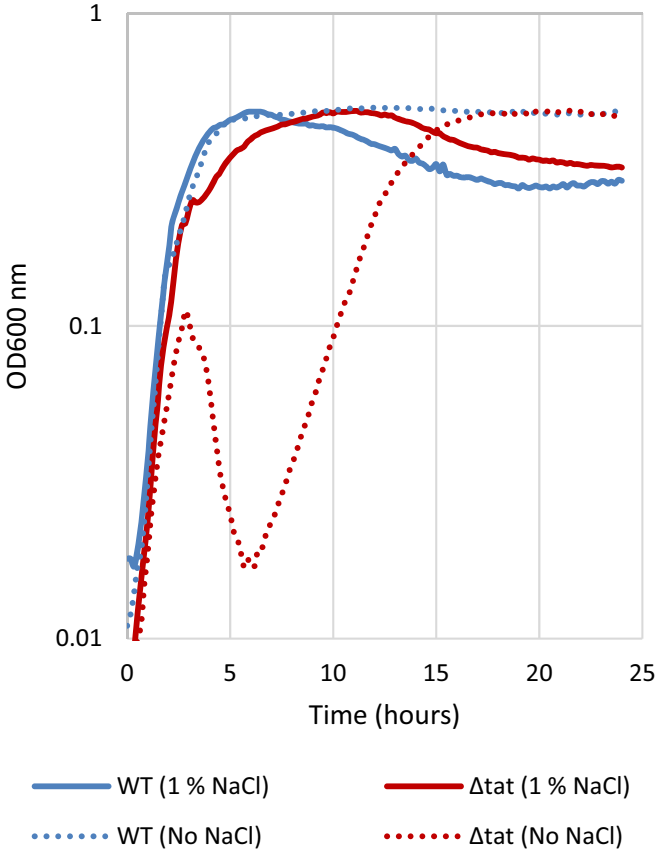

Fig. 2. Growth of the *B. subtilis* wild-type (WT) strain 168 and a total-*tat1* mutant (Δ*tat*) derivative strain in LB with or without 1% NaCl as monitored in a microtiter plate reader. In LB without NaCl, the Δ*tat* strain displays a lysis-recovery phenotype, which is typical for the growth of all *tat*-deficient *B. subtilis* strains [21,22]. Note that the bacteria grow to a lower OD_{600} in 96-well microtiter plates than in shake flasks (Fig. S1).

at 37 °C under vigorous shaking, or on LB agar plates at 37 °C. Growth in LB broth was recorded by optical density readings at 600 nm (OD_{600}). When appropriate the cultures were supplemented with antibiotics: 10 μg/mL tetracycline (Tc), 4 μg/mL phleomycin (Pl), 20 μg/mL kanamycin (Km) or 100 μg/mL spectinomycin (Sp) or combinations thereof.

2.2. Live/dead staining and fluorescence confocal microscopy

To monitor the viability of wild-type and *tat* mutant strains, they were first cultured overnight in 2 mL of LB with 1% NaCl and the appropriate antibiotics. The overnight cultures were diluted 50-fold into fresh 10 mL LB with 1% NaCl and grown till mid-exponential phase (approximately 3 h). A final 50-fold dilution was made in 75 mL LB without NaCl in in a 250 mL conical shake flask. During growth samples were withdrawn from the cultures for OD_{600} readings. *B. subtilis* strains equivalent to an OD_{600} of 1 were harvested at different time points and stained with the LIVE/DEAD BacLight™ Bacterial Viability Kit (ThermoFisher®) for 15 min according to the manufacturer's instructions. Essentially, this kit contains two dyes: the green-fluorescent nucleic acid stain SYTO9 that penetrates both viable and non-viable bacteria, and the red-fluorescent nucleic acid stain propidium iodide that penetrates only non-viable bacteria shifting the emitted fluorescence to red. LIVE/DEAD-stained bacteria were washed 1× with PBS to remove unbound dye and fixed in 4% formaldehyde for 10 min. Cells were spotted on a glass slide for microscopy. Image acquisition was performed with a Leica TCS SP8 fluorescence confocal microscope (Leica Microsystems, Germany). Images were processed using LAS X Life Science and ImageJ software (National Institutes of Health). Cells imaged in the two fluorescence channels were counted using the threshold and analyze particles ImageJ software plugins.

2.3. RNA extraction

For RNA extraction, the bacteria were cultured as described in Section 2.2. Total RNA was isolated from three independent cultures of wild-type or *tat* mutant *B. subtilis* cells, respectively, according to the method described by Eymann et al. with some modifications [16,23]. Briefly, bacterial cells equivalent to 15 OD_{600} units were harvested by centrifugation for 3 min at 4 °C after addition of ½ volume of ice-cold killing buffer (20 mM Tris/HCl [pH 7.5], 5 mM $MgCl_2$, 20 mM NaN_3) to the culture sample. After discarding the supernatant, cell pellets were frozen in liquid nitrogen and stored at −80 °C. For mechanical cell disruption, the pellets were resuspended in 200 μL of ice-cold killing buffer, immediately transferred to a Teflon disruption vessel (precooled and filled with liquid nitrogen), and then disrupted in a Mikro-Dismembrator S (Sartorius) for 2 min at 2600 rpm. The resulting frozen powder was resuspended in 4 mL of lysis solution prewarmed at 50 °C (4 M guanidine thiocyanate, 25 mM sodium acetate [pH 5.2], 0.5% N-laurylsarcosinate 40 [wt/vol]) by repeated pipetting. Afterwards, 1 mL aliquots of the lysate were transferred to microcentrifuge tubes and immediately frozen in liquid nitrogen. Total RNA was isolated by acid-phenol extraction. The samples were extracted twice with an equal volume of acid phenol/chloroform/isoamyl alcohol (25:24:1, [pH 4.5]) and once with chloroform/isoamyl alcohol (24:1). After adding 1/10 volume of 3 M sodium acetate (pH 5.2), RNA was precipitated with isopropanol, washed with 70% ethanol and dissolved in 100 μL of RNase free water. For transcriptome analysis, 35 μg RNA were DNase-treated using the RNase-Free DNase Set (Qiagen) and purified using the RNA Clean-Up and Concentration Kit (Norgen). The RNA concentration was measured using a NanoDrop spectrophotometer, and the quality of the RNA preparations was assessed using an Agilent 2100 Bioanalyzer according to the manufacturer's instructions.

2.4. Expression arrays

After quality control, 5 μg aliquots of the purified RNA were used for microarray analysis. Prior to cDNA synthesis, ten different in vitro synthesized transcripts derived from the One-Color RNA Spike-In kit (Agilent Technologies) were added in equal amounts to each total RNA sample [24]. The subsequent synthesis and fluorescent labeling of cDNA followed a strand-specific method using the FairPlay III Microarray Labeling Kit (Agilent Technologies) and actinomycin D (Calbiochem) [16]. 100 ng of Cy3-labeled cDNA were hybridized to the microarray following Agilent's hybridization, washing and scanning protocol (One-Color Microarray-based Gene Expression Analysis, version 5.5). Data were extracted and processed using the Feature Extraction software (version 11.5.1.1). For each gene, the median of the individual probe intensities was calculated and gene-level intensities were scaled, based on the intensity values of the ten different in vitro synthesized spike-in transcripts that hybridize to complementary control probes on the array. The average difference of the control signal intensities between different arrays was used to scale the intensities of each individual array in order to account for technical variation associated with sample processing. Further data analysis was performed using GeneSpring GX 14.8 software (Agilent Technologies) and R 3.5.2 [96]. The microarray data set is available from NCBI's Gene Expression Omnibus (GEO) database (accession number GSE149595). The scaled mRNA expression data are available as supplemental material (Supplementary Table S2, sheets 1 and 2). Voronoi treemap visualizations were generated after exporting the expression data to MS-Excel (MS-Office, Microsoft) using regulon information provided by the online resource SubtiWiki ([25,26]; http://subtiwiki.uni-goettingen.de/) [94] and the Voronoi treemap software (Decodon GmbH). In the treemaps thus generated, each individual cell represents an individual gene transcript and the color denominates the transcript level ratios between the wild-type and *tat* mutant bacteria.

2.5. Bacterial strain construction

B. subtilis IIG-Bs3 was made competent in Spizizen medium as previously described [27]. To introduce the *tatAyCy*::*spc* mutation in this strain, genomic DNA of *B. subtilis* 168 *tatAyCy*::*spc* was used as a template, and the *tatAyCy*::*spc* region was amplified by PCR with primers YdiG_F/YdiG_R that hybridize to the flanking regions of *tatAyCy* (Supplementary Table S3). Subsequently, the amplified DNA was used to transform competent cells of *B. subtilis IIG-Bs3* and transformants were selected on plates with Sp.

2.6. Growth of B. subtilis in microtiter plates

Strains were cultured overnight in 2 mL of LB with 1% NaCl and the appropriate antibiotics. The overnight cultures were diluted 50-fold into fresh 10 mL LB with 1% NaCl and grown till mid-exponential phase (approximately 3 h). A final 50-fold dilution was made into 100 μL of LB without NaCl in wells of a 96-well microtiter plate (Greiner), which was subsequently incubated in a Biotek Synergy II plate reader (37 °C, with shaking). OD_{600} readings were recorded at 10 min intervals for 24 h. For the growth studies with glucose supplementation, LB without NaCl containing 2% glucose was prepared by adding glucose from a 50% stock solution. For the growth studies with amino acid supplementation, stocks of 0.5 M of the amino acids arginine, glutamate or histidine were prepared in LB without NaCl and then filter-sterilized using a 0.2 μm membrane. The medium was then supplemented with the appropriate concentration of each amino acid.

2.7. LDS-PAGE and Western blotting

The cultures equivalent to 2.0 OD_{600} units were collected at two time points. A first sample was collected at the onset of lysis when the OD_{600} started to decline ($OD_{600} \sim 0.9$). Samples from parallel cultures of the *B. subtilis* 168 wild-type control strain growing in LB without NaCl were collected at essentially the same OD. The second time point of sampling was in the recovery phase when the OD_{600} of the cultures with *tat*

mutant or wild-type bacteria was ~2. The samples were centrifuged for 5 min at 14,000 rpm at 4 °C and then kept on ice. The supernatant was transferred to a separate eppendorf tube and proteins in this fraction were collected by precipitation with 10% trichloroacetic acid (TCA). To this end, the supernatant fractions were incubated with TCA on ice for 1 h. Subsequently, the precipitated proteins were collected by centrifugation for 10 min at 14,000 rpm, 4 °C. The supernatant was discarded and the pellet was washed with 500 µL of ice-cold acetone and centrifuged for 5 min at 14,000 rpm, 4 °C. Upon removal of the acetone supernatant, the protein pellet was dried at 60 °C for 10 min. Finally, 100 µL of lithium dodecyl sulphate (LDS) sample buffer with reducing agent (Life technologies) was added and the samples were incubated for 10 min at 95 °C. The collected cell pellets were resuspended in LDS sample buffer and, subsequently, the cells were disrupted with glass beads in a Precellys®24 homogenizer (3 × 30 s at 6500 rpm with 30 s intermittences). The samples were then heated to 95 °C for 10 min. Subsequently, samples with cellular or secreted proteins were separated by LDS-PAGE using pre-cast Bis-Tris NuPaGE gels (Invitrogen). The separated proteins were stained in the gel with SimplyBlue™ Safe Stain. Alternatively, the proteins separated by LDS-PAGE were semi-dry blotted (75 min at 1 mA/cm^2) onto a nitrocellulose membrane (Protran®, Schleicher & Schuell), and the presence of EfeB, FeuA, QcrA, Thioredoxin A (TrxA) and LiaH was detected with specific polyclonal antibodies raised in rabbits. Visualization of bound antibodies was performed with fluorescent IgG secondary antibodies (IRDye 800 CW goat anti-rabbit from Licor Biosciences) in combination with the Odyssey Infrared Imaging System (Licor Biosciences).

2.8. ICPMS

Wild-type and *tat* mutant bacteria were cultured in LB without NaCl as indicated above. Cells were harvested by centrifugation and the collected cell pellets were resuspended in Tris-HCl buffer (10 mM, pH 7.4) to 8 µL per OD_{600} per mL. After transfer of the sample to screw-capped micro tubes (Sarstedt, made from PP) filled with 0.5 mL glass beads (Sartorius, 0.1 mm diameter), the cells were disrupted by 6 cycles in a FastPrep-24 instrument (MP-Biomedicals; 30 s per cycle, 6.5 m/s, 4 min cooling on ice between the cycles). Glass beads and cell debris were removed by two subsequent centrifugation steps at 5000 x*g* for 5 min and at 20,000 x g for 10 min, and the supernatant from the last centrifugation step was stored at −20 °C in aliquots until further processing. Using size-exclusion chromatography (column: Superose 6 Increase 3.2 × 300, eluent: 10 mM Tris-HCl pH 7.4, flow rate: 100 µL/min, isocratic elution), aliquots from each sample were separated and the flow-through was directly injected into a 7500c ICP-MS (Agilent, plasma operated a 1460 W) to monitor the intensities for several elemental isotopes over a period of 100 min. The recorded chromatograms for each isotope were corrected for sensitivity drifts by a smoothed ^{13}C baseline, and the manufacturer provided natural isotope abundance using R scripts. Peak fitting and integration were performed with the program Fityk (version 1.3.1, [28]) and peak areas were normalized to the protein content of the sample as determined by Bradford assay using BSA as external calibrant.

3. Results and discussion

As shown in Fig. 2, *tat*-deficient *B. subtilis* cells that are introduced into LB without NaCl start to lyse after several hours of growth in LB lacking NaCl. To pinpoint the stage at which the bacteria actually start dying, we collected samples at different time points after diluting cells of the *B. subtilis* Δ*tat* mutant or the wild-type strain 168 in LB without NaCl. Cells in the collected samples were then stained with the fluorescent dyes SYTO9 and propidium iodide, which distinguishes living and dead cells by their green and red fluorescence, respectively (Fig. 3). The results obtained by confocal fluorescence microscopy showed that the *tat* mutant bacteria remained viable during the early time points after dilution into LB without NaCl, and that substantial numbers of dead bacteria were only detectable when the OD_{600} of the cultures with *tat* mutant bacteria started to decline at the entry into the lysis phase. In contrast, no dead bacteria were detectable when the wild-type bacteria were diluted into LB without NaCl (Fig. 3). Importantly, a fraction of the *tat* mutant bacteria remained viable during the lysis phase in LB without NaCl. Upon recovery, the *tat* mutant bacteria resumed growth and dead bacteria were no longer detectable.

To gain insights into the physiological state of *tat* mutant bacteria that start to lyse during growth in LB without NaCl, we recorded the growth of *B. subtilis* Δ*tat* in shake flasks and collected samples for RNA isolation at the moment when the OD_{600} of the cultures started to decline (OD_{600} ~ 0.9; Supplementary Fig. S1). Samples from parallel cultures of the *B. subtilis* 168 wild-type control strain in LB without NaCl were

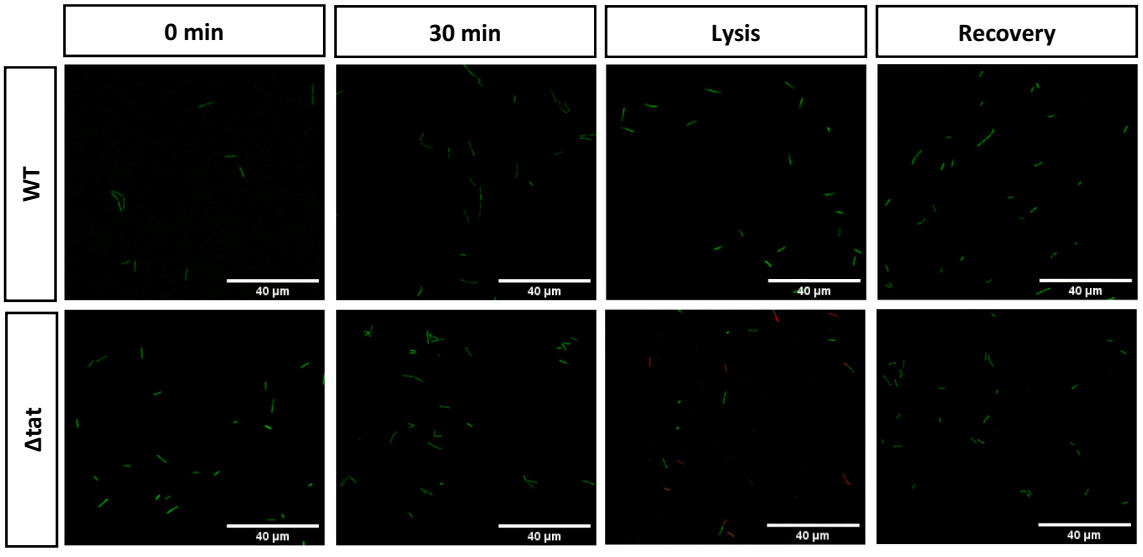

Fig. 3. Live/dead staining of *tat* mutant and wild-type bacteria upon dilution into LB without NaCl. The *B. subtilis* total-*tat1* mutant (Δ*tat*) and the wild-type strain *B. subtilis* 168 (WT) were grown in LB without NaCl. The bacteria were harvested immediately upon dilution into LB without NaCl (0 min), 30 min after dilution, upon entry into the lysis phase, and in the recovery phase. The harvested bacteria were stained with the SYTO9 and propidium iodide, and subsequently imaged by confocal fluorescence microscopy. The green fluorescence marks the living bacteria, while red fluorescence marks the dead bacteria.

A

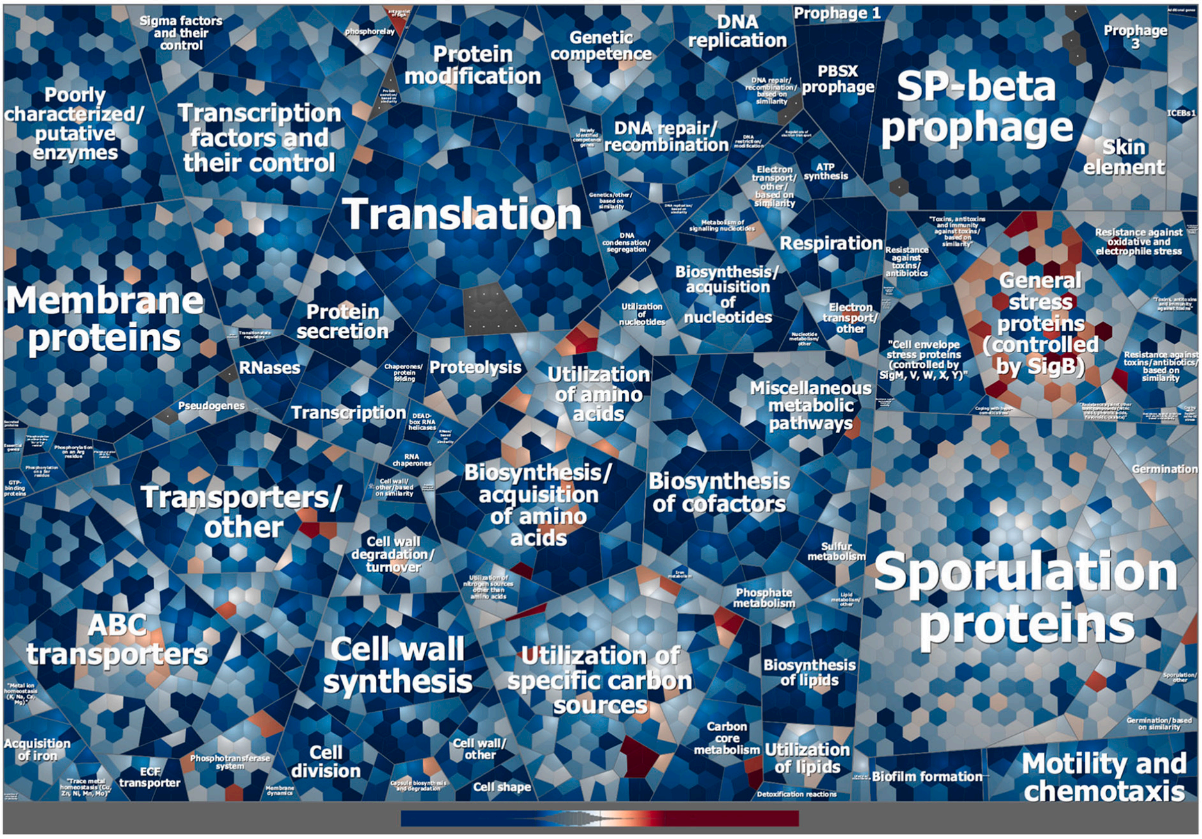
Sigma factors and their control
Poorly characterized/ putative enzymes
Transcription factors and their control
Protein modification
Genetic competence
DNA replication
Prophage 1
PBSX prophage
SP-beta prophage
Prophage 3
Skin element
DNA repair/ recombination
Translation
Respiration
Membrane proteins
Protein secretion
Biosynthesis/ acquisition of nucleotides
General stress proteins (controlled by SigB)
RNases
Proteolysis
Utilization of amino acids
Miscellaneous metabolic pathways
Pseudogenes
Transcription
Transporters/ other
Biosynthesis/ acquisition of amino acids
Biosynthesis of cofactors
Germination
Sporulation proteins
ABC transporters
Cell wall synthesis
Utilization of specific carbon sources
Biosynthesis of lipids
Acquisition of iron
Cell division
Utilization of lipids
Biofilm formation
Motility and chemotaxis

B


GlnR
CymR
AbrB_ repression
LexA_ repression
Rok
IolR
SigM
YlxR
SigG
Spo0A_ activation
Spo0A_ repression
SigV
PhoP_ activation
CcpA_ repression
SigA
SigB
SinR
PurR
ComK_ activation
SigL
SigF
SigX
GerE_ activation
CodY_ repression
SigK
Xpf
SigH
T-box
Fur
DegU_ repression
SigD
stringentresponse_ negativeregulation
SigE
SigW
ScoC
SigI
ComA

Fig. 4. Comparative transcriptome analysis of *B. subtilis* total-*tat1* (Δ*tat*) and the wild-type strain 168 in LB medium without NaCl. Voronoi treemaps are presented based on the functional classification of the transcripts of wild-type and *tat* mutant bacteria at the onset of lysis (A) and during the recovery phase (C). In addition, Voronoi treemaps based on the attribution of identified transcripts to regulons are shown for the onset of lysis (B) and during the recovery phase (D). Ratios of transcript levels in the wild-type and *tat* mutant bacteria in log2 were used to create the Voronoi treemaps. Each individual cell in the treemaps represents an individual gene transcript, and the color denominates the relative abundance of the individual transcript in the *tat* mutant bacteria compared to the wild-type strain. The respective fold-changes are presented in Supplementary Table S2. Supplementary Fig. S2 presents the same Voronoi treemaps, but with the name of each transcript written in the respective cell. The color red indicates transcript upregulation in *tat* mutant bacteria, and the color blue represents transcript downregulation in the *tat* mutant bacteria. Cells in dark grey represent mRNA transcripts that were not detected in the present expression array analysis. All transcript profiling experiments were performed in triplicate in independent cultures.

collected for RNA extraction at essentially the same OD. Upon processing of the RNA samples and appropriate quality control, transcript profiling was performed using expression arrays that represent all coding and non-coding genes of *B. subtilis* [16,29]. Further, we used spike-in normalization of in vitro synthesized RNA transcripts [24] for detailed comparisons of mRNA levels in the *tat* mutant bacteria and the wild-type control. This revealed a striking reorganization of the transcriptome in the *tat* mutant bacteria (Supplementary Table S2). As visualized through the Voronoi treemaps in Fig. 4 and Supplementary Fig. S2, the expression of many genes was strongly reduced in the *tat* mutant bacteria (depicted in blue) with only a specific subset of genes being upregulated (depicted in red). The upregulated genes relate to a limited number of regulons (Fig. 4B). The striking global downregulation observed in the *tat* mutant bacteria may relate to reduced transcription at the time point of sampling as the mutant bacteria had already ceased growth. The strong growth effect is also supported by a significant reduction in the expression of genes subject to the stringent response (Fig. 4B; Supplementary Fig. S2B).

3.1. Upregulation of oxidative stress-responsive genes in the lysis phase

The RNA polymerase sigma factor SigB is a key transcription factor that responds to various stress stimuli [30]. Upregulation was essentially only observed for the SigB-regulon in the *tat* mutant bacteria upon entering the lysis phase, which indicates exposure to severe stress. The strong 23-fold induction of the PerR-controlled *katA* gene encoding the major vegetative catalase that detoxifies H_2O_2, is in turn indicative of peroxide stress [31,95]. This view is supported by the 10-fold elevated transcript level of the *katE* gene for a second catalase of *B. subtilis* [32]. Likewise, the transcription of *ohrB* and *cypC*, two other SigB-controlled general stress genes, was also upregulated in the *tat* mutant bacteria. OhrB is known to confer hydroperoxide resistance in *B. subtilis* [33,34]. CypC is a long chain-fatty acid beta-hydroxylating cytochrome P450 that hydroxylates myristic acid to beta-hydroxymyristic acid by utilizing H_2O_2, and it is required for the protection against paraquat stress [35,36]. Altogether, the upregulation of *katA*, *katE*, *ohrB* and *cypC* at the start of the lysis phase is indicative of an accumulation of H_2O_2 and other reactive oxygen species (ROS) in the *tat* mutant bacteria. This is fully consistent with our previously reported observation that the TatAyCy-dependently exported EfeB protein consumes H_2O_2 for the conversion of ferric to ferrous iron, thereby also setting a limit to the unwanted production of reactive oxygen species by ferric iron-provoked Fenton chemistry [18]. It thus seems likely that the increased oxidative stress in the absence of TatAyCy or EfeB leads to the oxidation of phospholipids, which will affect membrane permeability and fluidity and ultimately leads to leakage and lysis of the cell [37]. Importantly, this view is consistent with the data presented in Fig. 3, where the increased membrane permeability is evidenced by the staining of *tat* mutant bacteria with the membrane-impermeable dye propidium iodide.

To verify the defective EfeB secretion at the onset of the lysis phase, Western blotting experiments were performed (Fig. 5). Indeed, at the beginning of the lysis phase, EfeB was not detectably secreted by the *tat* mutant bacteria, whereas the wild-type bacteria displayed low-level secretion of EfeB. Conversely, the *tat* mutant cells contained higher levels of EfeB than the wild-type cells, consistent with the previously reported EfeB secretion defect in the absence of a functional Tat machinery [11]. It thus seems that the *tat* mutant bacteria upregulated SigB-controlled genes for proteins that detoxify H_2O_2 in various ways, in order to mitigate the detrimental accumulation of H_2O_2 at the extracytoplasmic side of the membrane due to the absence of the peroxidase activity of EfeB. However, the Tat-deficiency may also elicit the production of ROS in other ways. For instance, one of the four known *B. subtilis* Tat substrates is the Rieske iron-sulfur protein QcrA. This protein is an integral component of the cytochrome bc_1 complex, which faces the extracellular side of the cytoplasmic membrane and serves as a menaquione:cytochrome *c* reductase [38]. It is thus conceivable that the absence of QcrA from the cytochrome bc_1 complex leads to imbalances in the respiratory chain and the formation of ROS. However, as shown by Western blotting (Fig. 5), the QcrA protein is barely expressed in growing wild-type *B. subtilis* at OD_{600} values equivalent to the lysis phase of the Δ*tat* mutant bacteria. Thus, it seems less likely that QcrA plays a role in the onset of the lysis phase.

3.2. Starvation responses upon entry of tat mutant bacteria into the lysis phase

The Voronoi treemaps of genome-wide gene expression in the lysis phase portray a global downregulation in the transcription of almost all systems in the *tat* mutant bacteria (Fig. 4). This includes many genes for nutrient uptake and central carbon metabolism, which could lead to starvation of the *tat* mutant bacteria due to an inability to acquire and utilize sugars. This view would be supported by the observation that the mutant bacteria substantially increased the expression of genes for amino acid catabolism in order to meet their energy demands. Indeed, the *tat* mutant bacteria seemed to utilize the cellular and extracellular arginine pools, as evidenced by a ~ 2.3- to 9-fold upregulation of the RocR-regulated *rocGABC* and *rocDEF* operons, which was one of the most prominent responses detected (Fig. 4A, B; Supplementary Fig. S2A, B; Supplementary Table S2). The *roc* operons encode proteins involved in catabolizing arginine to 2-oxaloglutarate [39]. Of note, the strong upregulation of the *roc* genes occurred despite the fact that expression of SR1, a small regulatory RNA that inhibits *ahrC* translation [40,41], was highly upregulated in the *tat* mutant bacteria. AhrC is a transcriptional regulator of the ArgR family, which represses the *arg* genes for arginine biosynthesis and activates the *roc* genes for arginine catabolism possibly via RocR and SigL [42–44].

The view that the *tat* mutant bacteria were starving and forced to utilize alternative sources for energy is further supported by the observed upregulation of CcpN-controlled *pckA* and *gapB* genes, which are both involved in gluconeogenesis. Also, the derepression of part of the CcpA regulon (e.g. *acoABCL*, *licBCAH*, *malA* and *glpFK*) indicates that the mutant cells experienced glucose limitation. In this respect, it should be noted that LB medium contains low amounts of glucose and other catabolite-repressing sugars, leading to repression of CcpA-dependent *B. subtilis* 168 genes especially in the exponential growth phase and the transition to stationary phase [16,45]. To verify the idea that the *tat* mutant bacteria were starving, we included 2% glucose in the LB medium without NaCl. As shown in Fig. 6, the lysis phenotype of the *tat*- mutant bacteria was suppressed by the glucose supplementation.

C

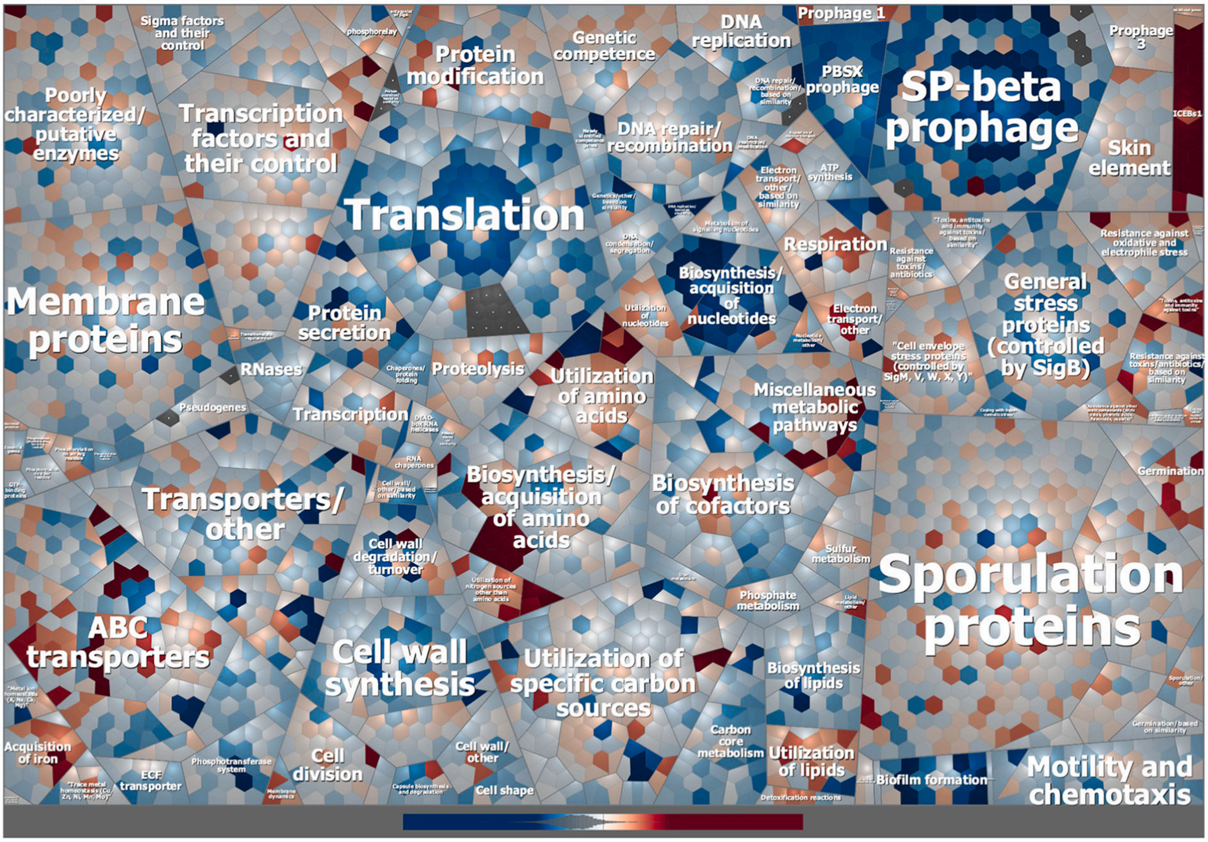

D

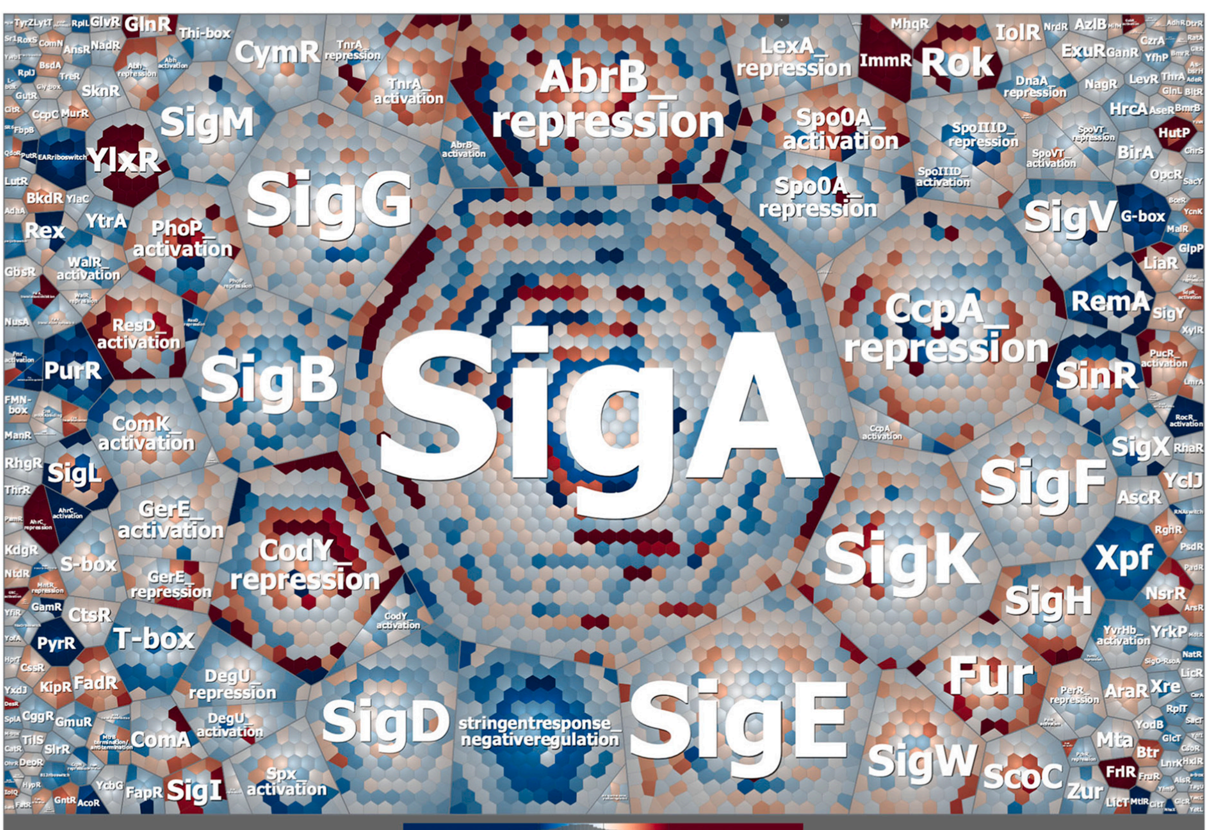

Fig. 4. (continued).

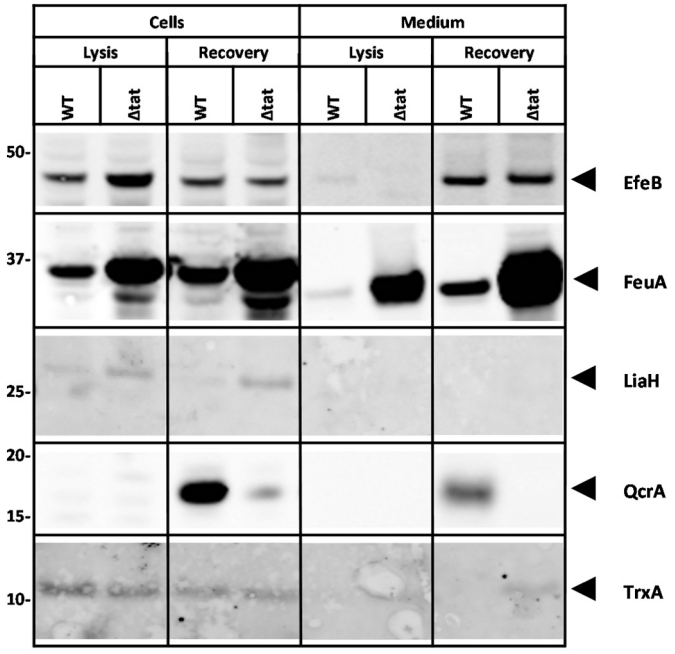

Fig. 5. Levels of cellular and secreted forms of the EfeB, FeuA, QcrA, LiaH and TrxA proteins in wild-type (WT) and total-*tat1* mutant (Δ*tat*) bacteria grown in LB medium without NaCl. Culture samples were collected and normalized to the respective OD_{600}. Subsequently, cells were separated from the growth medium by centrifugation. Cells were disrupted by bead-beating in LDS sample buffer. Proteins in the growth medium were collected by TCA precipitation. Subsequently, proteins from the cell and growth medium fractions were separated by LDS-PAGE. The presence of the EfeB, FeuA, QcrA, LiaH or TrxA proteins was visualized by Western blotting and immunodetection with specific polyclonal antibodies. The cytoplasmic TrxA protein of *B. subtilis* represents a sensitive marker for cell lysis [6,12]; QcrA is primarily a membrane protein but, in wild-type *B. subtilis*, a fraction of QcrA is known to be subject to cleavage by signal peptidase and subsequent secretion [19]. Please note that EfeB is secreted Tat-dependently in the lysis phase, but this Tat-dependency is lost in the recovery phase. The positions of molecular weight markers are indicated on the left of each panel (in kDa).

3.3. Oxidative stress is overcome in the recovery phase

To understand how the *tat* mutant cells overcame the problem imposed by impaired Tat-dependent protein translocation in the absence of NaCl, we also investigated the recovery phase by transcript profiling with expression arrays. The results are presented in Supplementary Table S2 and graphically depicted in Figs. 4C, D and Supplementary Figs. S2C, D. Contrary to the lysis phase, in the recovery phase the general downregulation of gene expression was no longer observed (Fig. 4), which is in agreement with the observation that the mutant cells had resumed growth (Fig. 2). Further, particular genes and regulons were upregulated, but these were mostly different from those in the lysis phase. A first important conclusion that can be reached from these observations is that the *tat* mutant bacteria no longer displayed the SigB- and PerR-dependent oxidative stress responses, despite the fact that EfeB most likely does not contribute to H_2O_2 detoxification in absence of a functional Tat translocase. There are various possible explanations for the alleviated oxidative stress response. For instance, the *spx* gene was upregulated, which is known to confer resistance to paraquat stress [46,47]. Likewise, the observed induction of *hpf* is suggestive of Hpf-medicated dimerization of ribosomes, which is a known resistance mechanism against paraquat-induced oxidative stress [36,48,49]. Also, the observed upregulation of the *liaI* and *liaH* genes may possibly facilitate LiaIH-mediated mitigation of membrane damage caused by the oxidative stress in absence of a functional Tat system. LiaH is a homologue of the phage shock protein A (PspA) of *E. coli* and the IM30

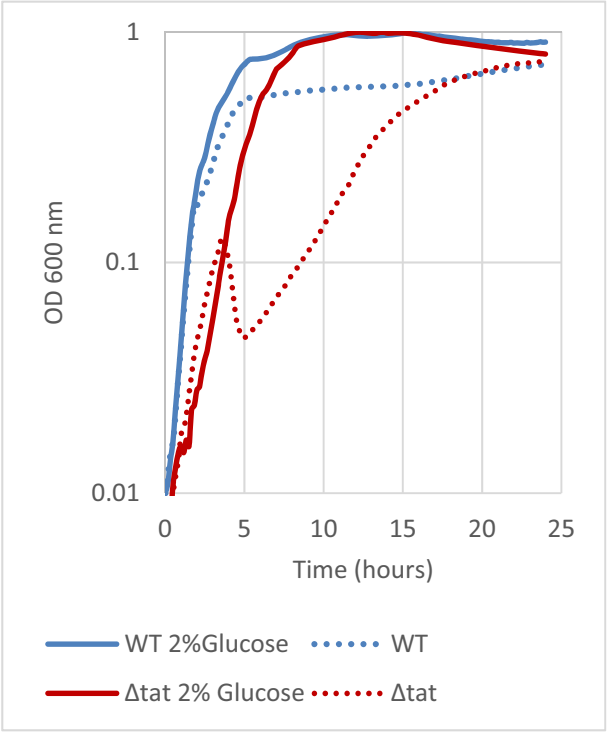

Fig. 6. Growth of *tat*-deficient *B. subtilis* in glucose-supplemented LB without NaCl. Growth of the *B. subtilis* total-*tat1* strain (Δ*tat*) and *B. subtilis* 168 (WT) in LB without NaCl was monitored in microtiter plates. Solid lines mark bacterial growth on medium supplemented with 2% glucose, and dotted lines mark growth on medium without glucose.

(VIPP1) protein of thylakoid-harboring organisms. Proteins of the PspA/IM30 family bind and stabilize distorted membrane regions [50–52]. The expression of LiaH is upregulated via the LiaRS two-component regulatory system upon cell envelope stresses elicited by antibiotics and antimicrobial peptides [53,54], secretion of certain heterologous proteins [95], and overexpression of the TatAyCy translocase to which it can bind [6]. Indeed, Western blotting showed that, in the recovery phase, the LiaH protein was upregulated in the *tat* mutant bacteria compared to the wild-type bacteria where LiaH was barely detectable (Fig. 5). This is different from the situation observed when *B. subtilis* is grown in regular LB with 1% NaCl, where the expression of LiaH is not influenced by the absence of a functional Tat system [6] and where no lysis-recovery growth phenotype is presented by *tat*-deficient bacteria (Fig. 2). Interestingly, the LiaH levels in the *tat* mutant bacteria grown in LB without NaCl were also slightly elevated compared to the wild-type bacteria at the entry into the lysis phase, despite the fact that in this phase a difference in *liaH* expression by the mutant and wild-type bacteria was not clearly evident by transcript profiling. In this respect, one has to bear in mind that mRNA levels in general were decreased in the *tat* mutant bacteria, thus likely facilitating increased translation of the remaining mRNA molecules present at similar levels as in the wild-type. Altogether, these findings imply that severe oxidative stress in the cell envelope due to the absence of a functional Tat system is a primary cause of the observed lysis phenotype of *tat* mutant *B. subtilis* cells upon growth in LB medium without NaCl, and that this stress is overcome in the recovery phase by various stress-mitigating systems. Further, membrane damage, as indicated by the upregulation of LiaH, would explain why the bacteria show symptoms of starvation upon entry into the lysis phase and start to utilize alternative energy sources.

3.4. Increased potential for uptake and biosynthesis of amino acids upon recovery

During the lysis phase, genes for catabolizing arginine and redirecting the metabolites for gluconeogenesis were significantly upregulated in the *tat* mutant bacteria. This was reversed in the recovery phase and, instead, the *artPQR* genes for uptake of arginine were upregulated 95- to 155-fold (Fig. 4), which encode a high-affinity arginine binding ABC transporter [55,56]. Alongside the enhanced potential for uptake of arginine, the capacity for biosynthesis of arginine was also dramatically upregulated as implied by increased expression of the CodY-regulated *arg* (*argBCDFGHJ*) and *car* (*carAB*) gene families [42,55,57,58]. Conversely, the *roc* genes for arginine utilization were downregulated [39,59]. All of this implies that the *tat* mutant cells had consumed their available arginine supply to survive the lysis phase and had started to replenish their arginine pool via increased uptake and biosynthesis of this amino acid. Furthermore, the *gltAB* genes for the biosynthesis of glutamate were also (~30-fold) upregulated in the recovery phase of the *tat* mutant cells, whereas in the wild-type cells *rocG* was more strongly expressed leading to low levels of *gtlAB* expression [60,61]. Lastly, the utilization and uptake of histidine was apparently upregulated in the recovering *tat* mutant bacteria, as indicated by the ~30-fold upregulation of the *hutPHUIGM* genes [62,63].

3.5. Iron starvation response during recovery

Despite the fact that the EfeUOB uptake system is unable to facilitate the utilization of ferric iron in *tat*-deficient *B. subtilis*, we did not observe an iron starvation response in the lysis phase (Fig. 4). However, a Fur-dependent iron starvation response was clearly evident in the recovery phase of the *tat* mutant cells, consistent with the impaired export of EfeB via the Tat pathway. This implies that, at the onset of lysis, the mutant bacteria still contained sufficient elemental iron, but that the cellular iron pool was rapidly depleted when the bacteria resumed growth. In particular, upon recovery the *ykuN* and *ykuP* genes were upregulated, both encoding FMN-binding flavodoxins. These proteins replace ferredoxin under conditions of iron limitation [64,65]. Likewise, systems for iron siderophore synthesis and uptake were also upregulated. For instance, the *dhbABCD* genes involved in synthesis of the siderophore bacillibactin were upregulated. Also, the transcriptional activator *btr* and its target, the *feuABC* operon for siderophore uptake, were upregulated [64,66–68]. The strong upregulation of *feuA* was confirmed by Western blotting, which showed that compared to the wild-type bacteria, indeed, the production of FeuA was strongly upregulated in the *tat* mutant bacteria upon recovery (Fig. 5). However, also in this case, the Western blotting detected upregulation of the FeuA levels in the *tat* mutant bacteria upon entry into the lysis phase, despite the fact that similar *feuA* mRNA levels were detected in the mutant and wild-type bacteria. Again, these data suggest that, due to the general depletion of mRNA in the mutant, similar *feuA* mRNA levels in the mutant and the wild-type bacteria gave raise to higher protein levels in the mutant bacteria, because the *feuA* mRNA was preferentially translated due to a lack of competition for ribosomes. Additionally, expression of *fbpB*, encoding a basic protein that acts as an RNA chaperone for the regulatory FsrA RNA in response to iron limitation was upregulated in the recovery phase, as was the case for the FsrA RNA itself [64,69,70]. All these adaptations seem to enable the *tat* mutant cells to overcome the iron limitation resulting from defective biogenesis of EfeB via Tat. However, quite remarkably, in the recovery phase we noticed the Tat-independent secretion of EfeB by *tat* mutant bacteria to levels that were comparable to the EfeB secretion by the wild-type bacteria (Fig. 5). Possibly, this Tat-independent secretion of EfeB relates to the fact that the expression level of genes for heme biosynthesis at the onset of the lysis phase was downregulated 20- to 30-fold. It is thus conceivable that the *tat* mutant cells that recovered from the lysis phase were depleted for heme and that there was insufficient heme to be bound by all EfeB molecules synthesized. As a result, the heme-deficient EfeB could become a substrate for the Sec pathway, which is known to accept loosely folded proteins for translocation [71]. This explanation would be supported by the finding that, despite the Tat-independent export of EfeB, the *tat* mutant cells displayed a strong induction of Fur-regulated genes in the recovery phase, which implies that EfeB was secreted in an inactive form. Likewise, we have previously shown that heterologous or hybrid Tat substrates were Sec-dependently secreted in *B. subtilis*, probably due to their inefficient folding in the cytoplasm and inadequate 'Sec-avoidance' [72,73]. However, it remains to be demonstrated whether the observed Tat-independent secretion of EfeB in the recovery phase is indeed facilitated by the Sec pathway.

3.6. Competition for nutrients induces genes for sibling killing and ICEBs genes during recovery

Amongst the most highly upregulated genes in the recovery phase of the *tat* mutant bacteria were the sibling killing genes *skfABC* (between 8- to 22-fold), the *alb* genes involved in production of the bacteriocin subtilosin (between 25- to 100-fold), and genes belonging to the so-called Integrative and Conjugative Elements of *B. subtilis* (*ICEBs1*) cluster (between 436- to 2000-fold). The upregulation of both the *skf* and *alb* genes was previously reported to occur upon increased competition for nutrients in a *B. subtilis* population [74,75]. Thus, the upregulation of the *skf* and *alb* genes in the recovery phase could be a consequence of the apparent starvation of the *tat* mutant bacteria upon entry into the lysis phase. The *ICEBs1* cluster consists of several genes regulated by ImmR, and it is involved in the transfer of mobile genetic elements [76–78]. In particular, the massive up to 2000-fold upregulation of the *ICEBs1* genes suggested that these genes might somehow be responsible for the recovery of the *tat* mutant bacteria. To investigate

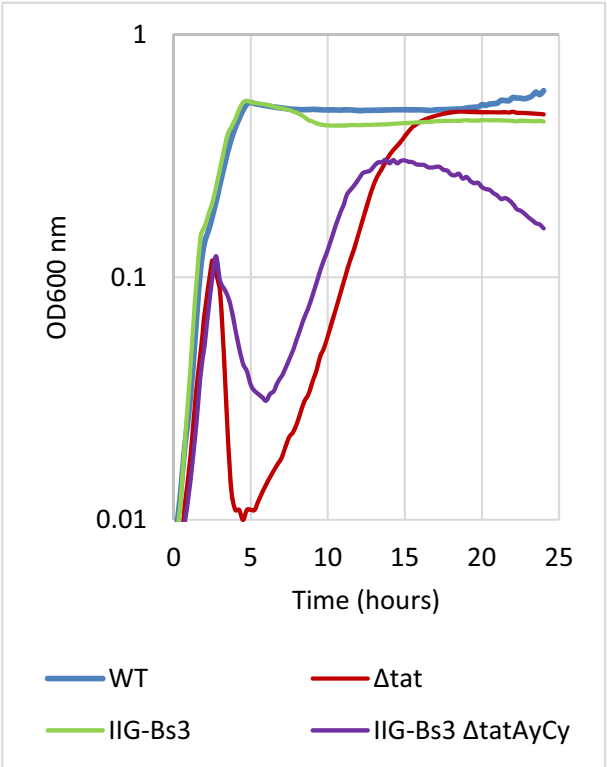

Fig. 7. Growth of *B. subtilis* cells lacking the *ICEBs1* genes in LB without NaCl. Growth of the *B. subtilis* strain IIG-Bs3, which lacks all *ICEBs1* genes, and the *tatAyCy* mutant derivative strain IIG-Bs3 Δ*tatAyCy* was monitored in microtiter plates. As a control, growth of the *B. subtilis* 168 strain (WT) and the *B. subtilis* total-*tat1* strain (Δ*tat*) was monitored in parallel.

whether induction of the ImmR regulon and the *ICEBs1* genes was responsible for recovery, the *tatAyCy* genes were deleted in a strain of *B. subtilis* lacking the *ICEBs1* genes. The mutant bacteria lacking both the *tatAyCy* and the *ICEBs1* genes (IIG-Bs3 Δ*tatAyCy*) still showed the lysis phenotype upon growth in LB without NaCl, whereas the mutant lacking just the *ICEBs1* genes (IIG-Bs3) grew similar to the wild-type (Fig. 7). Nevertheless, the mutant bacteria lacking both the *ICEBs1* genes and *tatAyCy* did not recover to the same extent as the *tat* mutant bacteria. These results indicate that the observed hyper-induction of *ICEBs1* genes was not a primary cause of recovery but, rather, that the *ICEBs1* genes may somehow assist the bacterial recovery.

3.7. Changes in the expression of several ABC transporters

While many transporter genes were downregulated at the entry into the lysis phase, the genes for various ABC transporters facilitating the uptake of nutrients and exchange of ions were found to be upregulated in the *tat* mutant bacteria during recovery. For instance, the CodY-

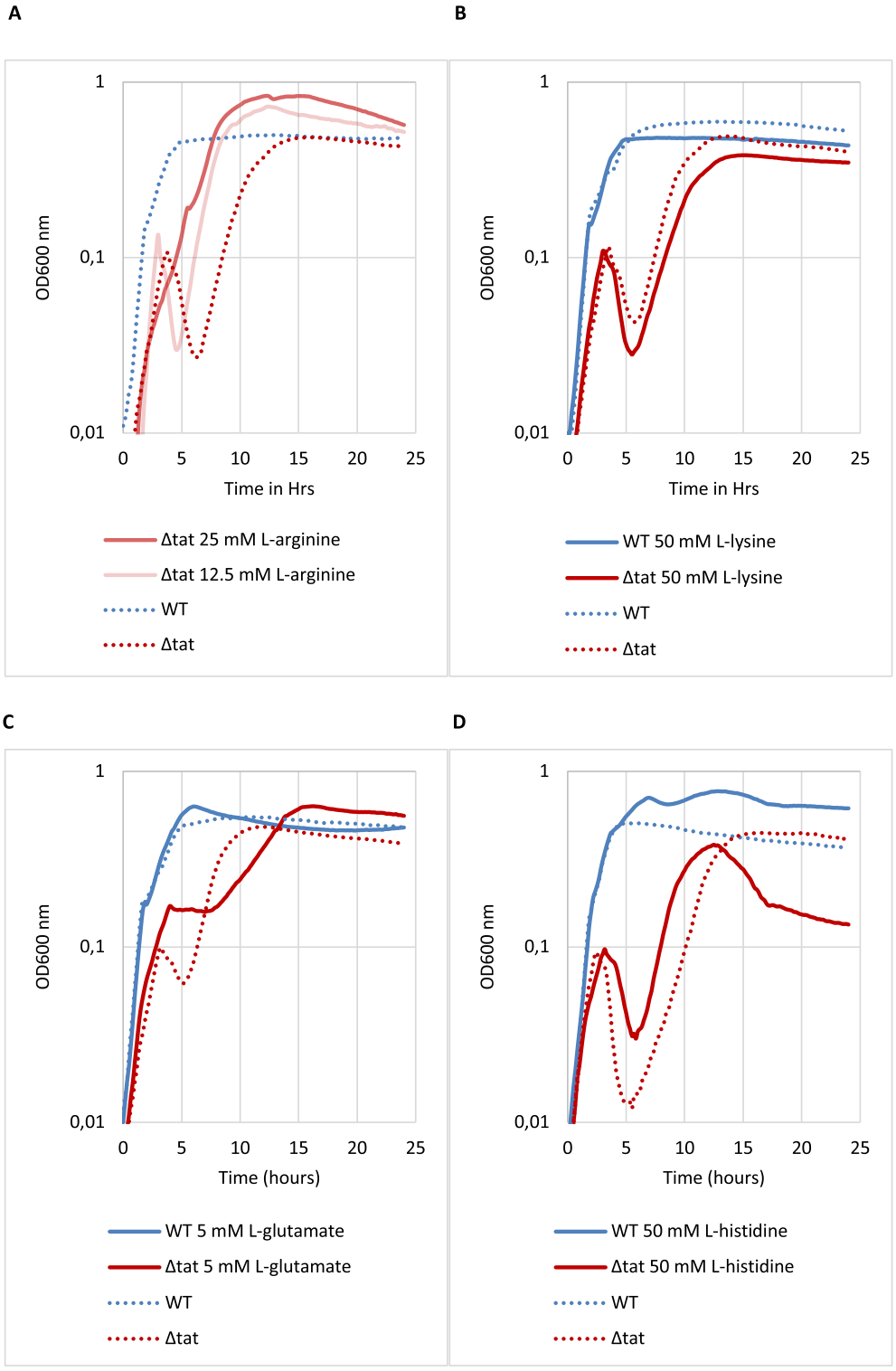

Fig. 8. Growth of *tat*-deficient *B. subtilis* in LB without NaCl, but supplemented with different amino acids. Growth of the *B. subtilis* total-*tat1* strain (Δ*tat*) and *B. subtilis* 168 (WT) in LB without NaCl was monitored in microtiter plates. The medium was supplemented with L-arginine (A), L-lysine (B), L-glutamate (C), or L-histidine (D) at the indicated concentrations. Solid lines mark bacterial growth on medium supplemented with the respective amino acid, dotted lines mark growth on medium without added amino acids.

regulated *frlBONMD* genes for fructose uptake and utilization were upregulated [79]. Thus, it seems that the internalized fructose is being converted to Glucose-6-Phosphate to be utilized as an energy source in the growing cells. Similarly, the *amyC* and *amyD* transcripts for melibose and rafinose transport were also upregulated upon recovery of the *tat* mutant bacteria [68]. Moreover, the *dct* operon involved in the uptake of other carbon sources, such as succinate, fumarate and oxaloacetate, was upregulated upon recovery of the *tat*-deficient cells. These observations are fully in line with the fact that the recovered cells were growing rapidly for which an adequate supply of nutrients is crucial.

3.8. Suppressed lysis phenotype upon arginine supplementation

As described above one of the most striking features displayed by *tat* mutant bacteria upon entry into the lysis phase was an extreme upregulation of the *roc* genes for arginine utilization, most likely as a starvation response due to oxidative damage of the cell membrane. Conversely, during the recovery phase the *roc* genes were no longer expressed at elevated level, whereas the genes for transport and synthesis of arginine were upregulated. These observations led us to investigate the effects of supplementation of the growth medium with this amino acid. To this end, LB medium without NaCl was supplemented with different amounts of L-arginine and the growth of the *tat*-deficient and wild-type bacteria on these supplemented media was recorded. Indeed, when the *tat*-deficient bacteria were supplemented with 25 mM L-arginine in LB without NaCl the lysis phenotype was completely suppressed (Fig. 8A). In fact, the growth of the *tat*-deficient bacteria was close to identical to that of the wild-type. Upon reduction of the L-arginine concentration to 12.5 mM, the protective effect of L-arginine against the lysis of the *tat*-deficient mutants in LB without NaCl was lost (Fig. 8A). In contrast to the supplementation with L-arginine, supplementation of LB with the control amino acid L-lysine did not alter the growth phenotype of the *tat* mutant bacteria on LB without NaCl (Figs. 8B). These results show that the availability of arginine modulates the growth behavior of *tat* mutant bacteria such that they do not display the typical lysis phase as observed upon growth in LB without NaCl. This finding supports the view that it is the consumption of arginine that is most important for survival of the lysis phase by a fraction of the *tat* mutant bacterial population. To obtain further evidence for the view that the elevated amino acid synthesis by the *tat* mutant bacteria in LB without NaCl contributes to their survival of the lysis phase, we inspected also their survival upon supplementation of this medium with L-glutamate or L-histidine. Indeed, when the *tat*-deficient bacteria received additional L-glutamate, there was a clear delay in the onset of the lysis phase and the decrease in OD_{600} during the lysis phase was less drastic (Fig. 8C). A similar but much milder effect was observed upon supplementation of the medium with 50 mM L-histidine (Fig. 8D). Taken together, these results imply that the increased propensity of the *tat* mutant bacteria for synthesis and/or uptake of arginine, glutamate and histidine as observed in the recovery phase is indeed required for their recovery. We presume that relatively high concentrations of these three amino acids had to be added to the medium to achieve recovery, because the *tat* mutant bacteria showed a clear down-regulation of genes for nutrient uptake in the lysis phase, including the *artPQR* genes for arginine uptake which were 8- to 10-fold downregulated (Supplementary Table S2). The same applied to the *gltT* gene for L-glutamate uptake (20-fold downregulated) and the *hutM* gene for histidine uptake (3–4-fold downregulated). Notably, supplementation experiments with other amino acids were not performed, because there were no substantial changes in the expression of the respective metabolic genes.

3.9. Restored Na^+ and K^+ homeostasis in the recovery phase

Importantly, apart from genes for the uptake and utilization of carbon sources, we also observed significant changes in the expression of genes for transporters of various metal ions in the *tat* mutant bacteria, including those for Na^+ and K^+ ions. Since the lysis phase is typical for *tat* mutant bacteria exposed to NaCl-depleted LB medium, this response was of interest. Therefore, we applied inductively coupled plasma mass spectrometry (ICP-MS), to measure the concentrations of Na^+ and K^+ ions in the wild-type and the *tat* mutant bacteria prior entry into the lysis phase and upon recovery.

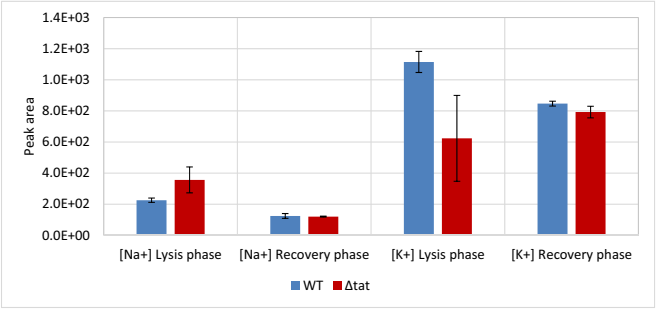

Fig. 9. Intracellular Na^+ and K^+ concentrations in *tat* mutant bacteria at the onset of the lysis phase and in the recovery phase during growth in LB without NaCl. The *B. subtilis* total-*tat1* strain (Δ*tat*) and *B. subtilis* 168 (WT) were grown in LB without NaCl, and samples for inductively coupled plasma mass spectroscopy (ICP-MS) were collected at the onset of the lysis phase and in the recovery phase, as indicated in Supplementary Fig. S1. The bar charts represent peak integrations of the areas under the curves obtained by ICP-MS.

As shown in Fig. 9, the *tat* mutant bacteria contained more intracellular Na^+ ions compared to the wild-type upon entry into the lysis phase. Consistent with this finding, the *mrpABCDEFG* genes, which encode the major Mrp sodium extrusion system of *B. subtilis* [80], were severely downregulated in the lysis phase. However, during recovery this difference in the cellular Na^+ concentration was ameliorated. Further, the expression of the Na^+/H^+ antiporter *nhaC* was consistently lower in the *tat*-deficient bacteria compared to the wild-type when grown in LB without NaCl [80,81]. Together, these observations suggest that the *tat*-deficient bacteria were less efficient compared to the wild-type in releasing the intracellular Na^+ when transferred from LB with 1% NaCl to LB medium without NaCl. Reducing the expression of *nhaC* when facing Na^+-deplete conditions is arguably an energetically favorable response, as the exchange of Na^+ against H^+ would result in a lowered proton-motive force (pmf) and, consequently, reduced generation of ATP by the pmf-dependent ATP synthase. During the recovery phase, the Na^+ concentrations in the *tat*-deficient and wild-type bacteria were comparable, in line with the view that the mutant bacteria had adapted to the absence of NaCl. Here, it is noteworthy that there was no significant change in the expression profiles of the genes involved in managing the bacterial Na^+ homeostasis upon recovery. In particular, the expression of the *mrp* and *nhaC* genes, and that of the *natAB* and *nhaC* genes for ATP-dependent Na^+ export systems showed no significant changes during the onset of lysis and the subsequent recovery phase [82,83]. This most likely means that, eventually, the remaining expression level of the Mrp and NhaC sodium transporters was sufficient to equilibrate the Na^+ level of the *tat* mutant bacteria to a similar extent as in the wild-type bacteria, or that there are other Na^+ transporters active in *B. subtilis* that remain to be discovered.

In contrast to the elevated Na^+ level, the *tat* mutant bacteria showed a lowered cellular K^+ concentration compared to the wild-type bacteria when entering the lysis phase. In agreement with this finding, upon entry into the lysis phase, expression of the *ydaO* riboswitch-controlled *ktrAB* and the recently discovered *kimA* genes for high-affinity K^+ uptake was severely downregulated (~25–30-fold) in the *tat* mutant bacteria compared to the wild-type [84,85]. Along with the *ktrAB* and *kimA* genes, the *ktrCD* genes encoding a low-affinity K^+ transporter and the *khtUT* genes encoding a K^+/H^+ antiporter were also slightly downregulated (~3-fold) in the *tat* mutant bacteria compared to the wild-type [80,85–88]. This suggests that, compared to the wild-type, the mutant

bacteria were less competent for K^+ intake upon entry into the lysis phase, which would lead to the lowered cellular K^+ concentration as observed.

Altogether, a depletion of the pmf in the *tat* mutant bacteria would provide a plausible explanation for the observed downregulation of most energy-consuming systems upon entry into the lysis phase. This view is in fact supported by the results of live/dead-staining, which showed that the membrane of a substantial part of the bacterial population entering the lysis phase had become permeable for propidium iodide (Fig. 3). In any case, in the surviving *tat* mutant cells that manage to recover from the lysis phase, the cellular Na^+ and K^+ concentrations are again comparable to those of the wild-type bacteria.

4. Conclusions

Altogether, our present findings show that *tat* mutant *B. subtilis* cells that are diluted into a NaCl-free growth medium have to face two major problems. Firstly, because they cannot secrete the heme peroxidase EfeB and perhaps also due to the mis-localization of the Rieske protein QcrA, these mutant cells suffer from severe oxidative stress at the membrane as evidenced by a strong upregulation of genes required for the detoxification of H_2O_2. This leads to their second major problem, namely the inability to take up nutrients, whereupon the cells start to starve. In response to this starvation, the *tat* mutant bacteria catabolize arginine and glutamate, leading to a further depletion of their intracellular nutrient pools and, ultimately, death of the largest part of the population. However, a sub-population manages to recover, probably because the respective cells are able to overcome severe oxidative stress at the membrane. Possibly, this sub-population mounts an adequate response earlier than the dying bacteria, allowing them to replenish their intracellular arginine and glutamate pools before starving to death. This view is supported by the observation that the lysis phase can be prevented by feeding the *tat* mutant bacteria arginine right from the moment when they are diluted into the NaCl-free medium. This observation focuses attention on the critical role played by arginine as a source of energy to overcome severe carbohydrate starvation. The idea that severe carbohydrate starvation is a major cause of death of a large part of the *tat* mutant population is strengthened by the observation that the lysis phase can be suppressed by the addition of an excess amount of glucose. Our present analysis does not give a direct answer to the question why the bacteria respond so strongly to the absence of a functional Tat machinery in the absence of NaCl in their growth medium. Nevertheless, there was a clear downregulation of the genes for Na^+ and K^+ transporters in the lysis phase. The lowered gene expression of the transporters could minimize an effect on the pmf, because the transport of sodium out of the cell and potassium into the cell requires a pmf. Hence, extrusion of sodium from the cytoplasm and import of potassium into the cells may have been lowered to minimize possible effects on the pmf. If so, the modulation of the Na^+ and K^+ transporters was insufficient and the resulting de-energization could in turn lead to a depletion of reducing power, for instance in the form of NADPH. This could result in a lowered ability to withstand oxidative stress. Irrespective of the precise mechanism, we conclude from our present observations that the *B. subtilis* Tat system has an important physiological function in protecting the cells against oxidative stress. This is particularly relevant in the natural habitat of *B. subtilis*, the soil and plant rhizosphere, where large fluctuations in the content of Na^+ and other ions may occur due to the ever-changing environmental conditions in general and rain or flooding in particular.

Supplementary data to this article can be found online at https://doi.org/10.1016/j.bbamcr.2020.118914.

Author contributions

B·P., U.M. and J.M.v.D. conceived and designed the experiments.
B.P., M.B·C., M.L.A., M.S., J.B., H.R., L.S., and U.M. performed experiments and analyzed the data.
D.B., U.V., U.M. and J.M.v.D. contributed strains and reagents.
U.V., U.M. and J.M.v.D. supervised the project.
B.P. and J.M.v.D. wrote the manuscript.
All authors have read and approved the manuscript.

CRediT authorship contribution statement

Bimal Prajapati: Conceptualization, Data curation, Formal analysis, Investigation, Methodology, Validation, Visualization, Writing – original draft, Writing – review & editing. **Margarita Bernal-Cabas:** Investigation, Methodology, Writing – review & editing. **Marina López-Álvarez:** Investigation, Methodology, Writing – review & editing. **Marc Schaffer:** Investigation, Methodology, Writing – review & editing. **Jürgen Bartel:** Data curation, Investigation, Methodology, Writing – review & editing. **Hermann Rath:** Data curation, Formal analysis, Software, Visualization, Writing – review & editing. **Leif Steil:** Data curation, Formal analysis, Software, Visualization, Writing – review & editing. **Dörte Becher:** Funding acquisition, Resources, Software, Writing – review & editing. **Uwe Völker:** Funding acquisition, Resources, Software, Supervision, Writing – review & editing. **Ulrike Mäder:** Conceptualization, Data curation, Formal analysis, Investigation, Methodology, Project administration, Resources, Software, Supervision, Validation, Visualization, Writing – review & editing. **Jan Maarten van Dijl:** Conceptualization, Formal analysis, Funding acquisition, Methodology, Project administration, Resources, Supervision, Writing – original draft, Writing – review & editing.

Declaration of competing interest

The authors declare that they have no known competing financial interests or personal relationships that could have appeared to influence the work reported in this paper.

Acknowledgements

This work was funded by the Graduate School of Medical Sciences [to B.P and M.B.C], the Ubbo Emmius Fund of the University of Groningen [to B.P.], the People Programme (Marie Skłodowska-Curie Actions) of the European Union's Horizon 2020 Programme under REA grant agreement numbers 642836 [to M.B.C., D.B. and J.M.v.D.] and 713660 [to M.L.A., and J.M.v.D.].

Data availability

The microarray data set is available from NCBI's Gene Expression Omnibus (GEO) database (accession number GSE149595).

References

[1] K.M. Frain, C. Robinson, J.M. van Dijl, Transport of folded proteins by the tat system, Protein J. 38 (4) (2019) 377–388.
[2] V.J. Goosens, J.M. van Dijl, Twin-arginine protein translocation, Curr Top Microbiol (2016) 69–94.
[3] D. Beck, N. Vasisht, J. Baglieri, C.G. Monteferrante, J.M. van Dijl, C. Robinson, C. J. Smith, Ultrastructural characterisation of *Bacillus subtilis* TatA complexes suggests they are too small to form homooligomeric translocation pores, Biochim. Biophys. Acta 1833 (8) (2013) 1811–1819.
[4] J. Fröbel, P. Rose, F. Lausberg, A.-S. Blümmel, R. Freudl, M. Müller, Transmembrane insertion of twin-arginine signal peptides is driven by TatC and regulated by TatB, Nat. Commun. 3 (2012) 1311.
[5] V.J. Goosens, A. De-San-Eustaquio-Campillo, R. Carballido-López, J.M. van Dijl, A tat ménage à trois — the role of *Bacillus subtilis* TatAc in twin-arginine protein translocation, Biochim. Biophys. Acta 1853 (10) (2015) 2745–2753.
[6] M. Bernal-Cabas, M. Miethke, M. Antelo-Varela, R. Aguilar Suárez, J. Neef, L. Schön, J.M. van Dijl, Functional association of the stress-responsive LiaH protein and the minimal TatAyCy protein translocase in Bacillus subtilis, Biochimica et Biophysica Acta - Mol Cell Res 1867 (8) (2020) 118719.
[7] B. Hou, E.S. Heidrich, D. Mehner-Breitfeld, T. Brüser, The TatA component of the twin-arginine translocation system locally weakens the cytoplasmic membrane of

Escherichia coli upon protein substrate binding, J. Biol. Chem. 293 (20) (2018) 7592–7605.
[8] R.M. Mould, C. Robinson, A proton gradient is required for the transport of two lumenal oxygen-evolving proteins across the thylakoid membrane, J. Biol. Chem. 266 (19) (1991) 12189–12193.
[9] T. Palmer, F. Sargent, B.C. Berks, Export of complex cofactor-containing proteins by the bacterial Tat pathway, Trends Microbiol. 13 (4) (2005) 175–180.
[10] M.-R. Yen, Y.-H. Tseng, E.H. Nguyen, L.-F. Wu, M.H. Saier, Sequence and phylogenetic analyses of the twin-arginine targeting (tat) protein export system, Arch. Microbiol. 177 (6) (2002) 441–450.
[11] J.D.H. Jongbloed, U. Grieger, H. Antelmann, M. Hecker, R. Nijland, S. Bron, J. M. Van Dijl, Two minimal tat translocases in Bacillus, Mol. Microbiol. 54 (5) (2004) 1319–1325.
[12] L. Krishnappa, A. Dreisbach, A. Otto, V.J. Goosens, R.M. Cranenburgh, C. R. Harwood, et al., Extracytoplasmic proteases determining the cleavage and release of secreted proteins, lipoproteins, and membrane proteins in *Bacillus subtilis*, J. Proteome Res. 12 (9) (2013) 4101–4110.
[13] I. Lüke, J.I. Handford, T. Palmer, F. Sargent, Proteolytic processing of *Escherichia coli* twin-arginine signal peptides by LepB, Arch of Microbiol 191 (12) (2009) 919–925.
[14] R.E. Dalbey, P. Wang, J.M. van Dijl, Membrane proteases in the bacterial protein secretion and quality control pathway, Microbiol. Mol. Biol. Rev. 76 (2) (2012) 311–330.
[15] J.D.H. Jongbloed, U. Martin, H. Antelmann, M. Hecker, H. Tjalsma, G. Venema, et al., TatC is a specificity determinant for protein secretion via the twin-arginine translocation pathway, J. Biol. Chem. 275 (52) (2000) 41350–41357.
[16] P. Nicolas, U. Mäder, E. Dervyn, T. Rochat, A. Leduc, N. Pigeonneau, et al., Condition-dependent transcriptome reveals high-level regulatory architecture in *Bacillus subtilis*, Science 335 (6072) (2012) 1103–1106.
[17] S. Eder, L. Shi, K. Jensen, K. Yamane, F.M. Hulett, A *Bacillus subtilis* secreted phosphodiesterase/alkaline phosphatase is the product of a Pho regulon gene, phoD, Microbiology 142 (8) (1996) 2041–2047.
[18] M. Miethke, C.G. Monteferrante, M.A. Marahiel, J.M. van Dijl, The *Bacillus subtilis* EfeUOB transporter is essential for high-affinity acquisition of ferrous and ferric iron, Biochim. Biophys. Acta 1833 (10) (2013) 2267–2278.
[19] V.J. Goosens, A. Otto, C. Glasner, C.C. Monteferrante, R. van der Ploeg, M. Hecker, et al., Novel twin-arginine translocation pathway-dependent phenotypes of *Bacillus subtilis* unveiled by quantitative proteomics, J. Proteome Res. 12 (2) (2013) 796–807.
[20] C.G. Monteferrante, M. Miethke, R. van der Ploeg, C. Glasner, J.M. van Dijl, Specific targeting of the metallophosphoesterase YkuE to the *Bacillus* cell wall requires the twin-arginine translocation system, J. Biol. Chem. 287 (35) (2012) 29789–29800.
[21] R. van der Ploeg, J.P. Barnett, N. Vasisht, V.J. Goosens, D.C. Pöther, C. Robinson, J. M. van Dijl, Salt sensitivity of minimal twin arginine translocases, J. Biol. Chem. 286 (51) (2011) 43759–43770.
[22] R. van der Ploeg, U. Mäder, G. Homuth, M. Schaffer, E.L. Denham, C. G. Monteferrante, et al., Environmental salinity determines the specificity and need for tat-dependent secretion of the YwbN protein in *Bacillus subtilis*, PLoS One 6 (3) (2011), e18140.
[23] C. Eymann, G. Homuth, C. Scharf, M. Hecker, *Bacillus subtilis* functional genomics: global characterization of the stringent response by proteome and transcriptome analysis, J. Bacteriol. 184 (9) (2002) 2500–2520.
[24] J. van de Peppel, P. Kemmeren, H. van Bakel, M. Radonjic, D. van Leenen, F.C. P. Holstege, Monitoring global messenger RNA changes in externally controlled microarray experiments, EMBO Rep. 4 (4) (2003) 387–393.
[25] R.H. Michna, B. Zhu, U. Mäder, J. Stülke, SubtiWiki 2.0—an integrated database for the model organism *Bacillus subtilis*, Nucleic Acids Res. 44 (D1) (2015) D654–D662.
[26] B. Zhu, J. Stülke, SubtiWiki in 2018: from genes and proteins to functional network annotation of the model organism *Bacillus subtilis*, Nucleic Acids Res. 46 (D1) (2017) D743–D748.
[27] J. Spizizen, Transformation of biochemically defficient strains of *Bacillus subtilis* by deoxyribonucleate, Proc. Natl. Acad. Sci. U. S. A. 44 (10) (1958) 1072–1078.
[28] M. Wojdyr, Fityk: a general-purpose peak fitting program, J. Appl. Crystallogr. 43 (5) (2010) 1126–1128.
[29] H. Rath, A. Reder, T. Hoffmann, E. Hammer, A. Seubert, E. Bremer, U. Völker, U. Mäder, Management of Osmoprotectant Uptake Hierarchy in *Bacillus subtilis* via a SigB-dependent antisense RNA, Front Microb 11 (2020) 622.
[30] M. Hecker, J. Pané-Farré, V. Uwe, SigB-dependent general stress response in *Bacillus subtilis* and related Gram-positive bacteria, Annu. Rev. Microbiol. 61 (1) (2007) 215–236.
[31] J. Mostertz, C. Scharf, M. Hecker, G. Homuth, Transcriptome and proteome analysis of *Bacillus subtilis* gene expression in response to superoxide and peroxide stress, Microbiol 150 (2) (2004) 497–512.
[32] S. Engelmann, M. Hecker, Impaired oxidative stress resistance of *Bacillus subtilis* sigB mutants and the role of katA and katE, FEMS Microbiol. Lett. 145 (1) (1996) 63–69.
[33] D.R. Cooper, Y. Surendranath, Y. Devedjiev, J. Bielnicki, Z.S. Derewenda, Structure of the *Bacillus subtilis* OhrB hydroperoxide-resistance protein in a fully oxidized state, Acta Crystallogr D Biol Crystallogr 63 (12) (2007) 1269–1273.
[34] M. Fuangthong, S. Atichartpongkul, S. Mongkolsuk, J.D. Helmann, OhrR is a repressor of ohrA, a key organic Hydroperoxide resistance determinant in *Bacillus subtilis*, J. Bacteriol. 183 (14) (2001) 4134–4141.
[35] D. Höper, U. Völker, M. Hecker, Comprehensive characterization of the contribution of individual SigB-dependent general stress genes to stress resistance of *Bacillus subtilis*, J. Bacteriol. 187 (8) (2005) 2810–2826.
[36] A. Reder, D. Höper, U. Gerth, M. Hecker, Contributions of individual B-dependent general stress genes to oxidative stress resistance of *Bacillus subtilis*, J. Bacteriol. 194 (14) (2012) 3601–3610.
[37] H. Mohan, K.U. Maheswari, A.K. Bera, G.K. Suraishkumar, Reactive oxygen species mediated modifications in *Bacillus subtilis* lipid membrane to improve protein productivities, Process Biochem. 45 (4) (2010) 467–474.
[38] J. Yu, L. Hederstedt, P.J. Piggot, The cytochrome bc complex (menaquinone: cytochrome c reductase) in *Bacillus subtilis* has a nontraditional subunit organization, J. Bacteriol. 177 (1995) 6751–6760.
[39] R. Gardan, G. Rapoport, M. Débarbouillé, Expression of the rocDEF operon involved in arginine catabolism in *Bacillus subtilis*, J. Mol. Biol. 249 (5) (1995) 843–856.
[40] N. Heidrich, A. Chinali, U. Gerth, S. Brantl, The small untranslated RNA SR1 from the *Bacillus subtilis* genome is involved in the regulation of arginine catabolism, Mol. Microbiol. 62 (2) (2006) 520–536.
[41] N. Heidrich, I. Moll, S. Brantl, In vitro analysis of the interaction between the small RNA SR1 and its primary target ahrC mRNA, Nucleic Acids Res. 35 (13) (2007) 4331–4346.
[42] L.G. Czaplewski, A.K. North, M.C.M. Smith, S. Baumberg, P.G. Stockley, Purification and initial characterization of AhrC: the regulator of arginine metabolism genes in *Bacillus subtilis*, Mol. Microbiol. 6 (2) (1992) 267–275.
[43] C.A. Dennis, N.M. Glykos, M.R. Parsons, S.E.V. Phillips, The structure of AhrC, the arginine repressor/activator protein from *Bacillus subtilis*, Acta Crystallogr D Biol Crystallogr 58 (3) (2002) 421–430.
[44] J.A. Garnett, F. Marincs, S. Baumberg, P.G. Stockley, S.E.V. Phillips, Structure and function of the arginine repressor-operator complex from *Bacillus subtilis*, J. Mol. Biol. 379 (2) (2008) 284–298.
[45] R. Detert Oude Weme, G. Seidel, O.P. Kuipers, Probing the regulatory effects of specific mutations in three major binding domains of the pleiotropic regulator CcpA of *Bacillus subtilis*, Front. Microbiol. 6 (2015) 1051.
[46] H. Schäfer, K. Turgay, Spx, a versatile regulator of the *Bacillus subtilis* stress response, Curr. Genet. 65 (4) (2019) 871–876.
[47] P. Zuber, management of oxidative stress in *bacillus*, ann rev microbiol 63 (1) (2009) 575–597.
[48] G. Akanuma, Y. Kazo, K. Tagami, H. Hiraoka, K. Yano, S. Suzuki, et al., Ribosome dimerization is essential for the efficient regrowth of *Bacillus subtilis*, Microbiology 162 (3) (2016) 448–458.
[49] A.K.W. Elsholz, K. Turgay, S. Michalik, B. Hessling, K. Gronau, D. Oertel, et al., Global impact of protein arginine phosphorylation on the physiology of *Bacillus subtilis*, Proc. Natl. Acad. Sci. U. S. A. 109 (19) (2012) 7451–7456.
[50] R. Manganelli, M.L. Gennaro, Protecting from envelope stress: variations on the phage-shock protein theme, Trends Microbiol. 25 (2017) 205–216.
[51] C. McDonald, G. Jovanovic, B.A. Wallace, O. Ces, M. Buck, Structure and function of PspA and Vipp1 N-terminal peptides: insights into the membrane stress sensing and mitigation, Biochim. Biophys. Acta Biomembr. 1859 (2017) 28–39.
[52] A. Thurotte, T. Brüser, T. Mascher, D. Schneider, Membrane chaperoning by members of the PspA/IM30 protein family, Commun. Integr. Biol. 10 (2017) 1–6.
[53] T. Mascher, S.L. Zimmer, T.A. Smith, J.D. Helmann, Antibiotic-inducible promoter regulated by the cell envelope stress-sensing two-component system LiaRS of *Bacillus subtilis*, Antimicrob. Agents Chemother. 48 (2004) 2888–2896.
[54] P.F. Popp, A. Benjdia, H. Strahl, O. Berteau, T. Mascher, The Epipeptide YydF intrinsically triggers the cell envelope stress response of *Bacillus subtilis* and causes severe membrane perturbations, Front. Microbiol. 11 (2020) 151.
[55] U. Mäder, G. Homuth, C. Scharf, K. Büttner, R. Bode, M. Hecker, Transcriptome and proteome analysis of *Bacillus subtilis* gene expression modulated by amino acid availability, J. Bacteriol. 184 (15) (2002) 4288–4295.
[56] Sekowska, A., Robin, S., Daudin, J.-J., Henaut, A., & Danchin, A. (2001). Extracting biological information from DNA arrays: an unexpected link between arginine and methionine metabolism in *Bacillus subtilis*. *Genome Biol, 2*(6), RESEARCH0019.
[57] A. Mountain, N.H. Mann, R.N. Munton, S. Baumberg, Cloning of a *Bacillus subtilis* restriction fragment complementing auxotrophic mutants of eight *Escherichia coli* genes of arginine biosynthesis, Mol. Gen. Genet. 197 (1) (1984) 82–89.
[58] M. O'Reilly, K. Woodson, B.C.A. Dowds, K.M. Devine, The citrulline biosynthetic operon, argC-F, and a ribose transport operon, rbs, from *Bacillus subtilis* are negatively regulated by Spo0A, Mol. Microbiol. 11 (1) (1994) 87–98.
[59] S. Calogero, R. Gardan, P. Glaser, J. Schweizer, G. Rapoport, M. Debarbouille, RocR, a novel regulatory protein controlling arginine utilization in *Bacillus subtilis*, belongs to the NtrC/NifA family of transcriptional activators, J. Bacteriol. 176 (5) (1994) 1234–1241.
[60] B.R. Belitsky, A.L. Sonenshein, Mutations in GltC that increase *Bacillus subtilis* gltA expression, J. Bacteriol. 177 (19) (1995) 5696–5700.
[61] D.E. Bohannon, A.L. Sonenshein, Positive regulation of glutamate biosynthesis in *Bacillus subtilis*, J. Bacteriol. 171 (9) (1989) 4718–4727.
[62] R.A. Bender, Regulation of the histidine utilization (hut) system in bacteria, Microbiol. Mol. Biol. Rev. 76 (3) (2012) 565–584.
[63] L.V. Wray Jr., S.H. Fisher, Analysis of *Bacillus subtilis* hut operon expression indicates that histidine-dependent induction is mediated primarily by transcriptional antitermination and that amino acid repression is mediated by two mechanisms: regulation of transcription initiation and inhibition of histidine transport, J. Bacteriol. 176 (17) (1994) 5466–5473.
[64] N. Baichoo, T. Wang, R. Ye, J.D. Helmann, Global analysis of the *Bacillus subtilis* Fur regulon and the iron starvation stimulon, Mol. Microbiol. 45 (6) (2002) 1613–1629.

[65] R.J. Lawson, C. von Wachenfeldt, I. Haq, J. Perkins, A.W. Munro, Expression and characterization of the two Flavodoxin proteins of *Bacillus subtilis*, YkuN and YkuP: biophysical properties and interactions with cytochrome P450 BioI†, Biochemistry 43 (39) (2004) 12390–12409.
[66] N. Bsat, J.D. Helmann, Interaction of *Bacillus subtilis* Fur (ferric uptake repressor) with the dhb operator in vitro and in vivo, J. Bacteriol. 181 (14) (1999) 4299–4307.
[67] A. Gaballa, J.D. Helmann, Substrate induction of siderophore transport in *Bacillus subtilis* mediated by a novel one-component regulator, Mol. Microbiol. 66 (1) (2007) 164–173.
[68] Y. Quentin, G. Fichant, F. Denizot, Inventory, assembly and analysis of *Bacillus subtilis* ABC transport systems, J. Mol. Biol. 287 (3) (1999) 467–484.
[69] H. Pi, J.D. Helmann, Sequential induction of Fur-regulated genes in response to iron limitation in *Bacillus subtilis*, Proc. Natl. Acad. Sci. U. S. A. 114 (48) (2017) 12785–12790.
[70] G.T. Smaldone, O. Revelles, A. Gaballa, U. Sauer, H. Antelmann, J.D. Helmann, A global investigation of the *Bacillus subtilis* Iron-sparing response identifies major changes in metabolism, J. Bacteriol. 194 (10) (2012) 2594–2605.
[71] J. Yuan, J.C. Zweers, J.M. van Dijl, R.E. Dalbey, Protein transport across and into cell membranes in bacteria and archaea, Cell. Mol. Life Sci. 67 (2) (2009) 179–199.
[72] M.A.B. Kolkman, R. van der Ploeg, M. Bertels, M. van Dijk, J. van der Laan, J. M. van Dijl, E. Ferrari, The twin-arginine signal peptide of *Bacillus subtilis* YwbN can direct either tat- or sec-dependent secretion of different cargo proteins: secretion of active Subtilisin via the *B. subtilis* Tat pathway, Appl and Environ Microbiol 74 (24) (2008) 7507–7513.
[73] R. van der Ploeg, C.G. Monteferrante, S. Piersma, J.P. Barnett, T.R.H.M. Kouwen, C. Robinson, J.M. van Dijl, High-salinity growth conditions promote tat-independent secretion of tat substrates in *Bacillus subtilis*, Appl. Environ. Microbiol. 78 (21) (2012) 7733–7744.
[74] J.E. González-Pastor, Cannibalism: a social behaviour in sporulating *Bacillus subtilis*, FEMS Microbiol. Rev. 35 (3) (2011) 415–424.
[75] G. Zheng, L.Z. Yan, J.C. Vederas, P. Zuber, Genes of the sbo-alb locus of *Bacillus subtilis* are required for production of the antilisterial bacteriocin subtilosin, J. Bacteriol. 181 (23) (1999) 7346–7355.
[76] J.M. Auchtung, C.A. Lee, K.L. Garrison, A.D. Grossman, Identification and characterization of the immunity repressor (ImmR) that controls the mobile genetic element ICEBs1 of *Bacillus subtilis*, Mol. Microbiol. 64 (6) (2007) 1515–1528.
[77] B. Bose, A.D. Grossman, Regulation of horizontal gene transfer in *Bacillus subtilis* by activation of a conserved site-specific protease, J. Bacteriol. 193 (1) (2010) 22–29.
[78] Baundauna Bose, J.M. Auchtung, C.A. Lee, A.D. Grossman, A conserved anti-repressor controls horizontal gene transfer by proteolysis, Mol. Microbiol. 70 (3) (2008) 570–582.
[79] V.M. Deppe, S. Klatte, J. Bongaerts, K.-H. Maurer, T. O'Connell, F. Meinhardt, Genetic control of Amadori product degradation in *Bacillus subtilis* via regulation offrlBONMD expression by FrlR, Appl. Environ. Microbiol. 77 (9) (2011) 2839–2846.
[80] T. Hoffmann, M. Bleisteiner, P.K. Sappa, L. Steil, U. Mäder, U. Völker, E. Bremer, Synthesis of the compatible solute proline by *Bacillus subtilis*: point mutations rendering the osmotically controlled proHJ promoter hyperactive, Environ. Microbiol. 19 (9) (2017) 3700–3720.
[81] Z. Prágai, C. Eschevins, S. Bron, C.R. Harwood, *Bacillus subtilis* NhaC, an Na^+/H^+ antiporter, influences expression of the *phoPR* operon and production of alkaline phosphatases, J. Bacteriol. 183 (2001) 2505–2515.
[82] J. Cheng, A.A. Guffanti, T.A. Krulwich, A two-gene ABC-type transport system that extrudes Na+ in *Bacillus subtilis* is induced by ethanol or protonophore, Mol. Microbiol. 23 (6) (1997) 1107–1120.
[83] Mitsuo Ogura, Kensuke Tsukahara, Kentaro Hayashi, Teruo Tanaka, The *Bacillus subtilis* NatK–NatR two-component system regulates expression of the natAB operon encoding an ABC transporter for sodium ion extrusion, Microbiology 153 (3) (2007) 667–675.
[84] K.F. Block, M.C. Hammond, R.R. Breaker, Evidence for widespread gene control function by the ydaO riboswitch candidate, J. Bacteriol. 192 (15) (2010) 3983–3989.
[85] J. Gundlach, C. Herzberg, D. Hertel, A. Thürmer, R. Daniel, H. Link, J. Stülke, Adaptation of *Bacillus subtilis* to life at extreme potassium limitation, MBio 8 (4) (2017) (e00861-17).
[86] M. Fujisawa, Y. Wada, M. Ito, Modulation of the K+ efflux activity of *Bacillus subtilis* YhaU by YhaT and the C-terminal region of YhaS, FEMS Microbiol. Lett. 231 (2) (2004) 211–217.
[87] G. Holtmann, E.P. Bakker, N. Uozumi, E. Bremer, KtrAB and KtrCD: two K+ uptake systems in *Bacillus subtilis* and their role in adaptation to hypertonicity, J. Bacteriol. 185 (4) (2003) 1289–1298.
[88] C. Lee, H.J. Kang, C. von Ballmoos, S. Newstead, P. Uzdavinys, D.L. Dotson, et al., A two-domain elevator mechanism for sodium/proton antiport, Nature 501 (7468) (2013) 573–577.
[89] V.J. Goosens, C.G. Monteferrante, J.M. van Dijl, The Tat system of Gram-positive bacteria, Biochim. Biophys. Acta 1843 (8) (2014) 1698–1706.
[94] SubtiWiki - a comprehensive knowledge base for Bacillus subtilis. (n.d.). Retrieved November 20, 2019, from http://subtiwiki.uni-goettingen.de/.
[95] H.L. Hyyryläinen, M. Sarvas, V.P. Kontinen, Transcriptome analysis of the secretion stress response of Bacillus subtilis, Appl. Microbiol. Biotechnol. 67 (3) (2005) 389–396, https://doi.org/10.1007/s00253-005-1898-1.
[96] R: The R Project for Statistical Computing (r-project.org).